observed below, but even above the saturation horizon, observable variations in species abundance can be attributed to subsurface respiration-driven dissolution, which is expected to be influenced by the overlying water ΔCO_3^{2-} (ref. 24). If carbonate-ion saturation had no effect on foraminifer abundance above the lysocline, we would expect a larger standard deviation in ΔCO_3^{2-} for estimates above the lysocline because faunally similar samples should be associated with a wider range of saturation levels. No such trend in the standard deviation is observed, supporting our assumption that faunal patterns above the lysocline are also associated with narrow (10 μmol kg^{-1}) ranges of ΔCO_3^{2-}. We note that the method seems to work in spite of regional variation in respiration-driven dissolution. Either these differences must be relatively small, or they are correlated with faunal assemblage.

Constraints on the method

In addition to the limitations of the method imposed by the uncertainty of the estimate, there are additional limitations imposed by the CLIMAP and modern analogue databases. From both the core-top and the CLIMAP LGM data sets, most of the samples are concentrated in the middle water column, with fewer at extreme high or low ΔCO_3^{2-} values. There are few core-top samples with ΔCO_3^{2-} higher than +60 μmol kg^{-1}, so we limit our reconstruction to samples deeper than 1,000 m, where we expect the ΔCO_3^{2-} to remain below 50 μmol kg^{-1}. Most of the CLIMAP LGM samples lie between 2,000–4,000 m.

Received 3 August 2001; accepted 9 January 2002.

1. Sanyal, A., Hemming, N. G., Hanson, N. & Broecker, W. S. Evidence for a higher pH in the glacial ocean from boron isotopes in foraminifera. *Nature* **373,** 234–236 (1995).
2. CLIMAP Project Members. Seasonal reconstruction of the Earth's surface at the last glacial maximum. *Geol. Soc. Am. Map Chart Ser.* **MC-36,** 1–18 (1981).
3. Mix, A. C. Influence of productivity variations on long-term atmospheric CO_2. *Nature* **337,** 541–544 (1989).
4. Ravelo, A. C., Fairbanks, R. G. & Philander, S. G. H. Reconstructing tropical Atlantic hydrography using planktonic foraminifera and an ocean model. *Paleoceanography* **5,** 409–431 (1990).
5. Prell, W. L. The stability of low-latitude sea-surface temperatures: An evaluation of the CLIMAP reconstruction with emphasis on the positive SST anomalies. (Report TR025, Department of Energy, Washington DC, 1985).
6. Millero, F. J. The effect of pressure on the solubility of minerals in water and seawater. *Geochim. Cosmochim. Acta* **46,** 11–22 (1982).
7. Mucci, A. The solubility of calcite and aragonite in seawater at various salinities, temperatures, and one atmosphere total pressure. *Am. J. Sci.* **283,** 780–799 (1983).
8. Duplessey, J. C. *et al.* Deep water source variations during the last climatic cycle and their impact on the global deep water circulation. *Paleoceanography* **3,** 343–360 (1988).
9. Oppo, D. W. & Horowitz, M. Glacial deep water geometry: South Atlantic benthic foraminiferal Cd/Ca and $\delta^{13}C$ evidence. *Paleoceanography* **15,** 147–160 (2000).
10. Yu, E.-F., Bacon, M. P. & Francois, R. Similar rates of modern and last glacial ocean thermohaline circulation inferred from radiochemical data. *Nature* **379,** 689–694 (1996).
11. Winguth, A., Archer, D. & Maier-Reimer, E. in *Inverse Methods in Global Biogeochemical Cycles* (eds Kasibhatla, P. *et al.*) (AGU Press, Washington DC, 2000).
12. Kennett, J. P. & Ingram, B. L. A 20,000 year record of ocean circulation and climate change from the Santa Barbara Basin. *Nature* **377,** 510–514 (1995).
13. Ganeshram, R. S., Pedersen, T. F., Calvert, S. E. & Murray, J. W. Large changes in oceanic nutrient inventories from glacial to interglacial periods. *Nature* **376,** 755–758 (1995).
14. Altabet, M. A., Francoise, R., Murray, D. M. & Prell, W. L. Climate-related variations in denitrification in the Arabian Sea from sediment $^{15}N/^{14}N$ ratios. *Nature* **373,** 506–509 (1995).
15. Archer, D., Winguth, A., Lea, D. & Mahowald, N. What caused the glacial/interglacial atmospheric pCO_2 cycles? *Rev. Geophys.* **38,** 159–189 (2000).
16. Farrell, J. W. & Prell, W. L. Climate change and $CaCO_3$ preservation: an 800,000 year bathymetric reconstruction from the central equatorial Pacific Ocean. *Paleoceanography* **4,** 447–466 (1989).
17. Peterson, L. C. & Prell, W. L. in *The Carbon Cycle and Atmospheric Carbon Dioxide: Natural Variations Archean to Present* (eds Sundquist, E. T. & Broecker, W. S.) 251–269 (American Geophysical Union, Washington DC, 1985).
18. Curry, W. B. & Lohmann, G. P. in *The Carbon Cycle and Atmospheric Carbon Dioxide: Natural Variations Archean to Present* (eds Sundquist, E. T. & Broecker, W. S.) 285–301 (American Geophysical Union, Washington DC, 1985).
19. Howard, W. R. & Prell, W. L. Late Quaternary $CaCO_3$ production and preservation in the Southern Ocean: Implications for oceanic and atmospheric carbon cycling. *Paleoceanography* **9,** 453–482 (1994).
20. Crowley, T. J. in *The Carbon Cycle and Atmospheric Carbon Dioxide: Natural Variations Archean to Present* (eds Sundquist, E. T. & Broecker, W. S.) 271–284 (American Geophysical Union, Washington DC, 1985).
21. Archer, D. & Maier-Reimer, E. Effect of deep-sea sedimentary calcite preservation on atmospheric CO_2 concentration. *Nature* **367,** 260–263 (1994).
22. Archer, D. An atlas of the distribution of calcium carbonate in deep sea sediments. *Glob. Biogeochem. Cycles* **10,** 159–174 (1996).
23. Overpeck, J. T., Webb, T. & Prentice, I. C. Quantitative interpretation of fossil pollen spectra: dissimilarity coefficients and the method of modern analogs. *Quat. Res.* **23,** 87–108 (1985).
24. Emerson, S. & Bender, M. L. Carbon fluxes at the sediment water interface of the deep sea: Calcium carbonate preservation. *J. Mar. Res.* **39,** 139–162 (1981).

Acknowledgements

We thank D. Lea, S. Lehman, R. Toggweiler and D. Sigman for helpful suggestions.

Correspondence and requests for materials should be addressed to D.M.A. (e-mail: dma@ngdc.noaa.gov).

Laser–Raman imagery of Earth's earliest fossils

J. William Schopf*, Anatoliy B. Kudryavtsev†, David G. Agresti†, Thomas J. Wdowiak† & Andrew D. Czaja*

* *Department of Earth & Space Sciences, and Institute of Geophysics & Planetary Physics (Center for the Study of the Evolution and Origin of Life), University of California, Los Angeles, California 90095-1567, USA*
† *Astro and Solar System Physics Program, Department of Physics, University of Alabama at Birmingham, Birmingham, Alabama 35294-1170, USA*

Unlike the familiar Phanerozoic history of life, evolution during the earlier and much longer Precambrian segment of geological time centred on prokaryotic microbes[1]. Because such microorganisms are minute, are preserved incompletely in geological materials, and have simple morphologies that can be mimicked by nonbiological mineral microstructures, discriminating between true microbial fossils and microscopic pseudofossil 'lookalikes' can be difficult[2,3]. Thus, valid identification of fossil microbes, which is essential to understanding the prokaryote-dominated, Precambrian 85% of life's history, can require more than traditional palaeontology that is focused on morphology. By combining optically discernible morphology with analyses of chemical composition, laser–Raman spectroscopic imagery of individual microscopic fossils provides a means by which to address this need. Here we apply this technique to exceptionally ancient fossil microbe-like objects, including the oldest such specimens reported from the geological record, and show that the results obtained substantiate the biological origin of the earliest cellular fossils known.

Over the past few decades, the rules for accepting ancient microfossil-like objects as *bona fide* Precambrian fossils have become well established. Such objects should be demonstrably biogenic, and indigenous to and syngenetic with the formation of rocks of known provenance and well-defined Precambrian age[2,4,5]. Of these criteria, the most difficult to satisfy has proved to be biogenicity, in particular for the notably few fossil-like objects reported from Archaean (>2,500 million years (Myr) old) deposits[2,4]—the putative biological origin of which has been beset by controversy[2,6–8]. This difficulty has been obviated in part by analyses of the isotopic composition of carbon in coexisting inorganic (carbonate) minerals and in whole-rock acid-resistant carbonaceous residues (kerogens), which have been used to trace the isotopic signature of biological (photoautotrophic) carbon fixation to at least ~3,500 Myr ago[9]. But because investigations of such bulk kerogen samples yield only an average value of the materials analysed, they cannot provide information about the biogenicity of individual minute objects that are claimed to be fossil.

Significant progress toward solving this problem has been made by using an ion microprobe to analyse the carbon isotopic composition of single Precambrian microfossils[10]. Laser–Raman spectroscopic imagery of ancient individual fossil microbes provides a means by which to extend available analytical data to a molecular level. In a previous study[11], we applied this technique to analyses *in situ* of Eocene fossil wood and Precambrian microscopic organic-walled fossils, and showed that it can provide insight into the molecular make-up and the fidelity of preservation of the kerogenous matter of which such fossils are composed. Because Raman spectroscopy is non-intrusive, non-destructive and particularly sensitive to the distinctive carbon signal of carbonaceous (kerogenous) organic matter, it is an ideal technique for such studies. Here we have used this technique to investigate graphitic, geochemically highly altered, dark brown to black carbonaceous filaments that have been inferred to be remnants of especially

© 2002 Macmillan Magazines Ltd

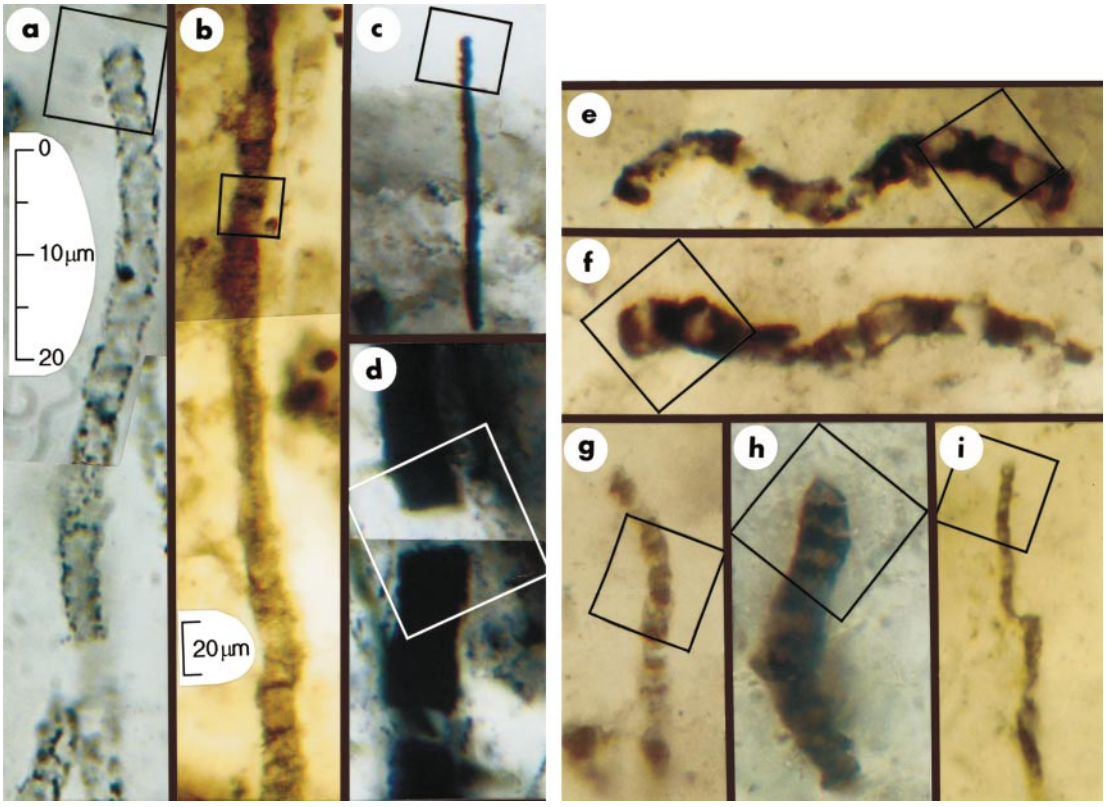

Figure 1 Optical photomicrographs showing carbonaceous (kerogenous) filamentous microbial fossils in petrographic thin sections of Precambrian cherts. Scale in **a** represents images in **a** and **c**–**i**; scale in **b** represents image in **b**. All parts show photomontages, which is necessitated by the three-dimensional preservation of the cylindrical sinuous permineralized microbes. Squares in each part indicate the areas for which chemical data are presented in Figs 2 and 3. **a**, An unnamed cylindrical prokaryotic filament, probably the degraded cellular trichome or tubular sheath of an oscillatoriacean cyanobacterium, from the ~770-Myr Skillogalee Dolomite of South Australia[12]. **b**, *Gunflintia grandis*, a cellular probably oscillatoriacean trichome, from the ~2,100-Myr Gunflint Formation of Ontario, Canada[13]. **c**, **d**, Unnamed highly carbonized filamentous prokaryotes from the ~3,375-Myr Kromberg Formation of South Africa[14]: the poorly preserved cylindrical trichome of a noncyanobacterial or oscillatoriacean prokaryote (**c**); the disrupted, originally cellular trichomic remnants possibly of an *Oscillatoria*- or *Lyngbya*-like cyanobacterium (**d**). **e**–**i**, Cellular microbial filaments from the ~3,465-Myr Apex chert of northwestern Western Australia: *Primaevifilum amoenum*[4,5], from the collections of The Natural History Museum (TNHM), London, specimen V.63164[6] (**e**); *P. amoenum*[4] (**f**); the holotype of *P. delicatulum*[4,5,15], TNHM V.63165[2] (**g**); *P. conicoterminatum*[5], TNHM V63164[9] (**h**); the holotype of *Eoleptonema apex*[5], TNHM V.63729[1] (**i**).

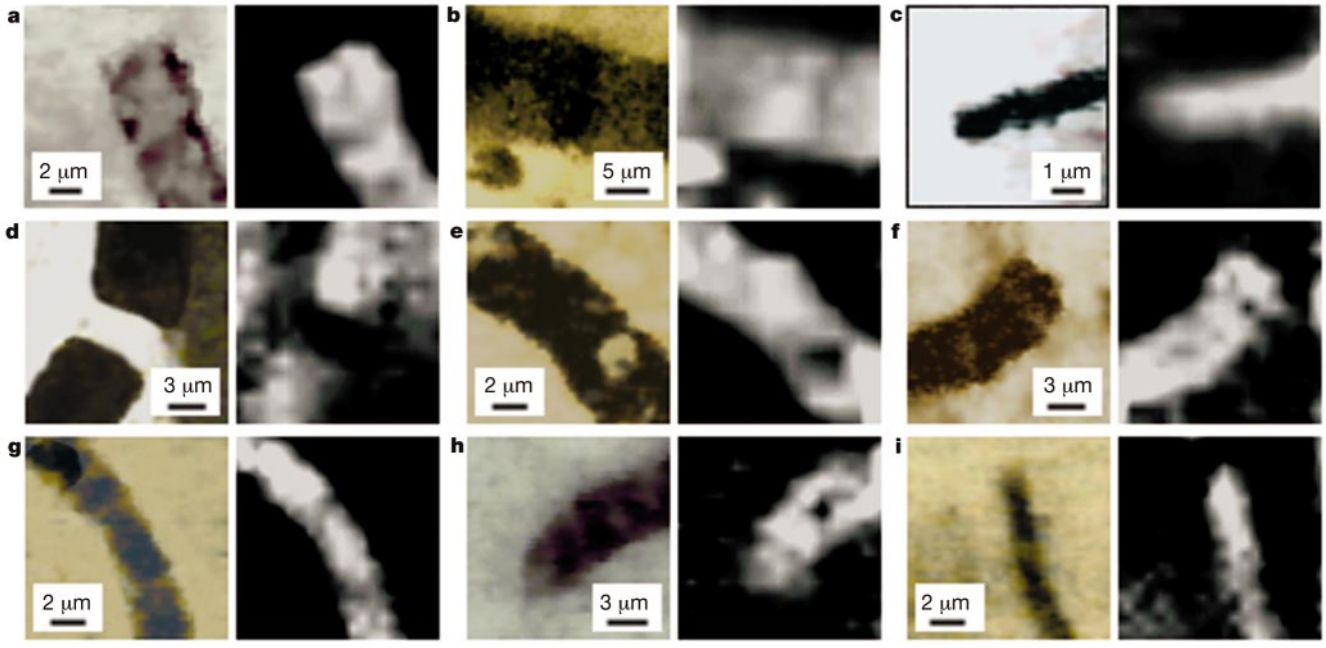

Figure 2 Digital optical images and corresponding Raman images. **a**–**i**, Optical images (left) and Raman 'G' band intensity maps (right), of areas of fossils indicated by the squares in Fig. 1a–i, respectively.

© 2002 Macmillan Magazines Ltd

ancient microbes, and show that laser–Raman spectroscopic imagery can provide powerful evidence of the biogenicity of even such poorly preserved microstructures, including those regarded to be the oldest known fossils.

We analysed microbial fossil filaments that had been three-dimensionally permineralized in cryptocrystalline cherts from one subgreenschist facies (Gunflint Formation) and three geochemically more altered (greenschist facies) Precambrian geological units: (1) a cylindrical prokaryotic filament (Fig. 1a) from a domical stromatolite of the ~770-Myr Skillogalee Dolomite of South Australia[12]; (2) a cellular trichome (Fig. 1b) from a domical stromatolite of the ~2,100-Myr Gunflint Formation of Ontario, Canada[13]; (3) two prokaryotic filaments (Fig. 1c, d) from flat-laminated microbial mats of the ~3,375-Myr Kromberg Formation of South Africa[14]; and (4) the oldest fossils known—five specimens (Fig. 1e–i) representing 4 of 11 described taxa[4,5] of cellular microbial filaments permineralized in organic-rich clasts of the ~3,465-Myr Apex chert of northwestern Western Australia[4,5,15]. The range of Raman spectra obtained from fossil microbes and associated organic detritus petrified in 24 Precambrian cherts including that preserved in less geochemically altered units, and the correlation of such spectra with H/C ratios measured in bulk-sample kerogens and their relevance to processes of organic metamorphism will be described elsewhere (J.W.S. *et al.*, manuscript in preparation).

Together with optical (Fig. 1) and Raman (Fig. 2) images of fossils analysed from the four geological units, we present in Fig. 3 the dominant features of their Raman spectra: vibrational bands at ~1,350 cm^{-1} and ~1,600 cm^{-1}, which are characteristic of carbonaceous (kerogenous) materials and commonly designated 'D' (disordered) and 'G' (graphitic), respectively, because of their presence in various forms of graphite[16].

The results establish the kerogenous composition of the microscopic structures studied. Raman spectra also show that the filaments are embedded in fine-grained quartz and are devoid of virtually all other mineral phases that are identifiable by Raman analysis[17,18]. As shown by the similarity of the spectra obtained from fossils preserved in geochemically highly altered units, for example, ~770 Myr (Fig. 3a), ~3,375 Myr (Fig. 3c, d) and ~3,465 Myr (Fig. 3e–i), the graphite-like character of the kerogen signature is related to the fidelity of preservation rather than to geological age.

The kerogen signal is not a result of contamination by the immersion oil used to enhance the optical image of some specimens, as is evident by comparing the spectra of filaments both without (Fig. 3a, b, upper panels) and with (Fig. 3a, b, lower panels) an overlying veneer of oil, as well as by the prominent kerogen signal of numerous specimens measured in the absence of such oil (for example, Fig. 3e, f, h). Indeed, not only is the Raman spectrum of the immersion oil (Fig. 3j) easily distinguishable from the kerogen signal of the fossils (for example, by the presence in the oil spectrum of major bands at ~1,000 cm^{-1} and ~1,450 cm^{-1}) but, because the confocal capability of the analytical system allowed a vertical resolution of 1–3 μm of the signals acquired, precise focusing of the laser permitted exclusion of spectral contributions from this potential contaminant.

Similarly, the kerogen signal is not a result of contamination from graphitic (no. 2) pencil markings used in the past to encircle the Apex fossils (Fig. 1e–i) to indicate their locations. Such markings are no longer present, having been cleaned thoroughly from the upper surfaces of the Apex thin sections, and the Raman signature of pencil lead, characterized by a small broad 'D' band and a major and exceedingly sharp 'G' band[17], is easily distinguishable from the signature of kerogen. In addition, rather than being exposed at upper surfaces of thin sections, the fossils studied are enclosed completely in the embedding quartz matrix and therefore have been analysed at depths (measured optically to be as much as 65 μm) in the sections where they are demonstrably not affected by surface contamination.

Finally, by correlating directly molecular composition with filament morphology, the Raman images (Fig. 2) establish unequivocally that the specimens shown are composed of carbonaceous (graphitic) kerogen and that this organic matter is present in the fossils in concentrations much greater than those in the wispy, mucilage-like clouds of finely divided particulate kerogen in which fossils of each of the four deposits are preserved.

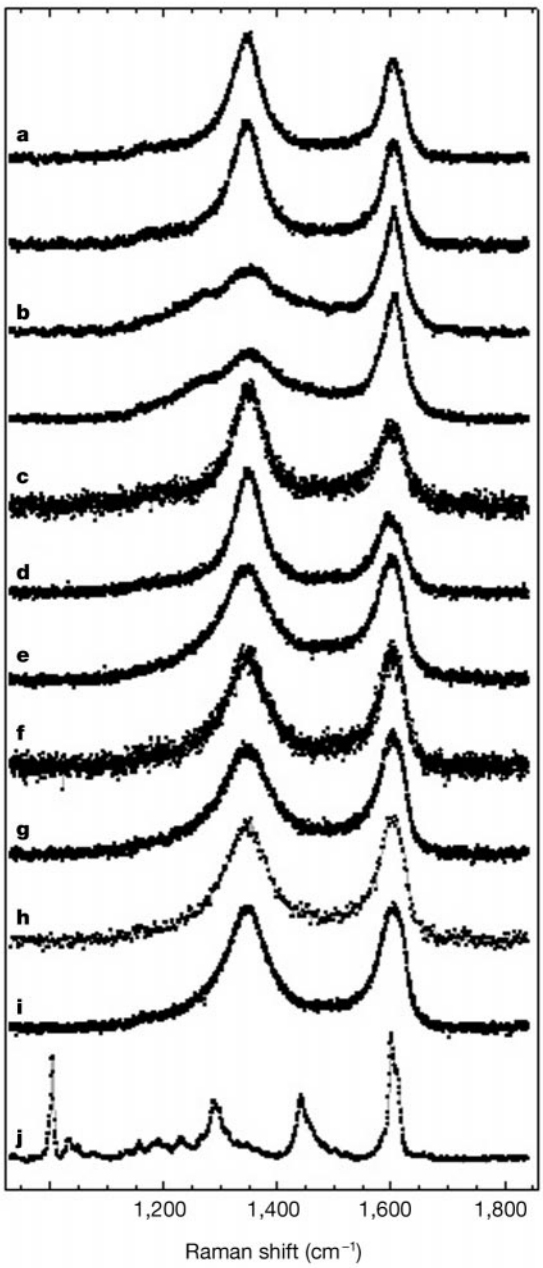

Figure 3 Typical spectral bands of parts of fossils shown in Fig. 1 used for Raman imaging (Fig. 2) and the spectrum of immersion oil used to enhance the optical image of some specimens. **a**, **b**, Point spectra of the Skillogalee filament shown in Fig. 1a, without (above) and with (below) a covering veneer of immersion oil; and of *Gunflintia grandis* (Fig. 1b), without (above) and with (below) an oil veneer (showing a broad 'D' band and its substructure, typical of the kerogen in this relatively unmetamorphosed, subgreenschist facies, geologic unit). **c**–**i**, Point spectra of other fossils from which Raman images were acquired: unnamed filamentous prokaryotes from the Kromberg Formation (**c**, **d**; shown in Fig. 1c, d, respectively); cellular filamentous prokaryotes from the Apex chert (**e**–**i**; shown in Fig. 1e–i, respectively). **j**, Spectrum of immersion oil used to enhance the optical image of some specimens.

© 2002 Macmillan Magazines Ltd

Our data show that, applied to exceedingly ancient and geochemically highly altered (graphitic, carbonized) kerogenous microscopic fossils, Raman imagery can be used to correlate directly chemical composition with optically discernible morphology and to prove the presence of crucial indicators of biogenicity, such as kerogenous cell walls. When applied to particularly poorly preserved fossil-like microscopic filaments, for which optical microscopy can only hint at cellularity (Fig. 1a, c, d), this highly sensitive technique can yield convincing evidence of biogenicity. Most notably, by providing a means by which to correlate biologically characteristic (kerogenous) composition with features of morphology that typify filamentous microbes—such as cylindrical (Fig. 1a–i), sinuous (Fig. 1a, e, f, h) and tapering (Fig. 1e, f, h) filament form, and the presence of transverse cell walls (Fig. 1b, e–i) and distinctively shaped terminal cells (Fig. 1e, f, h)—optical microscopy (Fig. 1) coupled with laser–Raman imagery (Fig. 2) and measurement of Raman point spectra (Fig. 3) substantiates the biological origin of the oldest putative fossils now known (Fig. 1e–i). By the time of preservation of the diverse, exceptionally ancient, microscopic filaments of the Apex chert[4,5], ~3,500 Myr ago, microbial life was flourishing and presumably widespread. □

Methods

Optical photomicrography

We acquired the optical photomicrographs (Fig. 1) in transmitted white light with a Leitz Orthoplan 2 automatic photomicroscope.

Raman spectroscopy

Laser–Raman spectroscopic data (Figs 2 and 3) were obtained with a Dilor XY (formerly Instruments S.A., now J.Y. Horiba) 0.8-m triple-stage system that has macro-, micro- and confocal line-scan imaging options. This system permitted acquisition of both individual point spectra, typically over a period of 100 s, and true Raman images that show the spatial distribution of molecular components. The confocal capability of the system was such that we could use a 100× objective without immersion oil (having an extended working distance of 3.4 mm and a numerical aperture of 0.8) to obtain all Raman data with a planar resolution of < 1 μm and a vertical resolution of 1–3 μm. Laser wavelengths ranging from blue to infrared were provided by a coherent krypton ion laser equipped with appropriate optics. We used a wavelength of 531 nm (in the green portion of the spectrum) typically at a laser power of less than 8 mW over a 1-μm spot—an instrumental configuration that we showed to be well below the threshold that results in radiation damage to the specimens analysed.

Fossil specimens situated in the uppermost ~65 μm of petrographic thin sections were centred in the path of the laser beam projected through an Olympus BX40 microscope. The upper surfaces of thin sections were either polished (with a paste containing 1-μm-sized diamonds) or unpolished and finished by a slurry of 600 mesh carborundum. To enhance the optical image of specimens situated more than ~10 μm below the upper surface of unpolished sections, we covered the area imaged by a thin veneer (~1-μm thick) of type B non-drying microscopy immersion oil (R. P. Cargille Laboratories). Not only have appropriate analyses (see above) shown that the presence of this thin veneer has no appreciable effect on the Raman spectra acquired, but the point spectra of specimens in polished sections (for example, Fig. 1a, b) and of most specimens (12/23) analysed in unpolished sections (for examples, Fig. 1e, f, h) were obtained without this veneer.

Raman imaging

To acquire Raman images (Fig. 2), a rectangular area enclosing a part of a fossil was selected for imaging, the backscattered Raman spectra obtained in each rectangle were collected through the optical system described above along micrometre-resolution scan lines, and their x–y registrations were automatically recorded to provide a pixel-assigned array of spectral elements ('spexels')[11]. A typical Raman image comprised 25 × 25 spectral elements, each analysed for 5–10 s, resulting in a total data collection time of 50–100 min for each image. We processed the several hundred spexels for each specimen by constructing a map of the intensity in the spectral window corresponding either to the 'D' band (at ~1,350 cm^{-1}) or the 'G' band (~1,600 cm^{-1}) of the kerogenous material; maps made by the 'G' band were generally of relatively higher Raman image quality. The resulting 'chemical image' shows the areal distribution of the fossil structures that produced the Raman spectral bands originating from specific molecular components.

Received 3 July; accepted 30 November 2001.

1. Schopf, J. W. in *The Proterozoic Biosphere, A Multidisciplinary Study* (eds Schopf, J. W. & Klein, C.) 587–593 (Cambridge Univ. Press, New York, 1992).
2. Schopf, J. W. & Walter, M. R. in *Earth's Earliest Biosphere, Its Origin and Evolution* (ed. Schopf, J. W.) 214–239 (Princeton Univ. Press, Princeton, 1983).
3. Mendelson, C. V. & Schopf, J. W. in *The Proterozoic Biosphere, A Multidisciplinary Study* (eds Schopf, J. W. & Klein, C.) 865–951 (Cambridge Univ. Press, New York, 1992).
4. Schopf, J. W. in *The Proterozoic Biosphere, A Multidisciplinary Study* (eds Schopf, J. W. & Klein, C.) 25–39 (Cambridge Univ. Press, New York, 1992).
5. Schopf, J. W. Microfossils of the Early Archean Apex chert: new evidence of the antiquity of life. *Science* **260,** 640–646 (1993).
6. Buick, R. Carbonaceous filaments from North Pole, Western Australia: are they fossil bacteria in Archean stromatolites? *Precambrian Res.* **24,** 157–172 (1984).
7. Awramik, S. M., Schopf, J. W. & Walter, M. R. Carbonaceous filaments from North Pole, Western Australia: are they fossil bacteria in Archean stromatolites? A discussion. *Precambrian Res.* **39,** 303–309 (1988).
8. Buick, R. Carbonaceous filaments from North Pole, Western Australia: are they fossil bacteria in Archean stromatolites? A reply. *Precambrian Res.* **39,** 311–317 (1988).
9. Hayes, J. M., Des Marais, D. J., Lambert, I. B., Strauss, H. & Summons, R. E. in *The Proterozoic Biosphere, A Multidisciplinary Study* (ed. Schopf, J. W. & Klein, C.) 81–134 (Cambridge Univ. Press, New York, 1992).
10. House, C. H. *et al.* Carbon isotopic composition of individual Precambrian microfossils. *Geology* **28,** 707–710 (2000).
11. Kudryavtsev, A. B., Schopf, J. W., Agresti, D. G. & Wdowiak, T. J. *In situ* laser–Raman imagery of Precambrian microscopic fossils. *Proc. Natl Acad. Sci. USA* **98,** 823–826 (2001).
12. Schopf, J. W. & Fairchild, T. R. Late Precambrian microfossils: a new stromatolitic microbiota from Boorthanna, South Australia. *Nature* **242,** 537–538 (1973).
13. Barghoorn, E. S. & Tyler, S. A. Microorganisms from the Gunflint chert. *Science* **147,** 563–577 (1965).
14. Walsh, M. M. & Lowe, D. R. Filamentous microfossils from the 3,500-Myr-old Onverwacht Group, Barberton Mountain Land, South Africa. *Nature* **314,** 530–532 (1985).
15. Schopf, J. W. & Packer, B. M. Early Archean (3.3-billion to 3.5-billion-year-old) microfossils from Warrawoona Group, Australia. *Science* **237,** 70–73 (1987).
16. Tuinstra, F. & Koenig, J. L. Raman spectra of graphite. *J. Chem. Phys.* **53,** 1126–1130 (1970).
17. Williams, K. P. J., Nelson, J. & Dyer, S. *The Renishaw Raman Database of Gemological and Mineralogical Materials.* (Renishaw Tranducers Systems Division, Gloucestershire, England, 1997).
18. McMillan, P. F. & Hofmeister, A. M. Infrared and Raman spectroscopy. *Rev. Mineral.* **18,** 99–159 (1988).

Acknowledgements

We thank M. Walsh for loan of the Kromberg specimens; The Natural History Museum, London, for loan of the Apex specimens; and J. Shen-Miller for manuscript review. This work was supported by grants from the JPL/CalTech Astrobiology Center (to J.W.S.) and from the National Aeronautics and Space Administration Exobiology Program (to T.J.W.). A.D.C. is an NSF predoctoral Fellow. The Raman imaging facility at the University of Alabama at Birmingham is a consequence of the vision of L. DeLucas.

Correspondence and requests for materials should be addressed to J.W.S. (e-mail: schopf@ess.ucla.edu).

Questioning the evidence for Earth's oldest fossils

Martin D. Brasier*, Owen R. Green*, Andrew P. Jephcoat*, Annette K. Kleppe*, Martin J. Van Kranendonk†, John F. Lindsay‡, Andrew Steele§ & Nathalie V. Grassineau‖

* *Earth Sciences Department, University of Oxford, Parks Road, Oxford OX1 3PR, UK*
† *Geological Survey of Western Australia, 100 Plain Street, East Perth, Western Australia, 6004, Australia*
‡ *Research School of Earth Sciences, Australian National University, Canberra ACT 0200, Australia*
§ *School of Earth, Environmental and Physical Sciences, University of Portsmouth, Burnaby Road, Portsmouth PO1 3QL, UK*
‖ *Department of Geology, Royal Holloway University of London, Egham Hill, Surrey TW20 0EX, UK*

Structures resembling remarkably preserved bacterial and cyanobacterial microfossils from ~3,465-million-year-old Apex cherts of the Warrawoona Group in Western Australia[1–4] currently provide the oldest morphological evidence for life on Earth and have been taken to support an early beginning for oxygen-producing photosynthesis[5]. Eleven species of filamentous prokaryote, distinguished by shape and geometry, have been put forward as meeting the criteria required of authentic Archaean micro-

© 2002 Macmillan Magazines Ltd

Copyright © 2002 EBSCO Publishing